Ferroptosis-Related lncRNAs Signature is a Prognostic Factor in Hepatocellular Carcinoma: A Study Based on TCGA Data

Xiangjin Hu
Capital Medical University https://orcid.org/0000-0002-0117-0883
Sailun Wang
Capital Medical University
Jia Guo
Capital Medical University
Fang Xiong
Capital Medical University
Jun Lv (junlu9876@126.com)
Capital Medical University

Research

Keywords: lncRNAs, HCC, prognosis, ferroptosis, immunotherapy, FRLS

Posted Date: September 20th, 2021

DOI: https://doi.org/10.21203/rs.3.rs-847334/v1

Abstract

Background Hepatocellular carcinoma (HCC) is the most common type of liver cancer and is the fourth leading cause of cancer-related death worldwide. Ferroptosis is a form of iron-dependent programmed cell death, and is characterized by intracellular accumulation of reactive oxygen species (ROS). Long non-coding RNAs (lncRNAs), as valuable prognostic factors for HCC patients, play a vital role in regulating ferroptosis.

Methods RNA-sequencing datasets and ferroptosis-related genes were retrieved from The Cancer Genome Atlas (TCGA) database and the Molecular Signature Database. we performed Pearson correlation analysis between the lncRNAs and ferroptosis-related genes, and subsequently used regression analysis (univariate Cox analysis, multivariate Cox regression analysis, and Lasso regression analysis) to screen the ferroptosis-related lncRNAs with prognostic value in HCC, the prognostic ferroptosis-related lncRNAs signature (FRLS) was finally constructed. In addition, we reevaluated the model in terms of survival, clinical characteristics, and immune microenvironment.

Results Univariate Cox regression analysis revealed 34 differently expressed ferroptosis-related lncRNAs related to the prognosis of HCC. Among them, 12 ferroptosis-related lncRNAs (LUCAT1, LINC01224, THUMPD3-AS1, AC116025.2, LINC00942, SNHG10, AC131009.1, POLH-AS1, MKLN1-AS, LINC01138, LNCSRLR, AL031985.3) were regarded as independent prognosis predictors of HCC, and were incorporated into the construction of the prognostic FRLS. Patients were divided into two groups based on the prognostic FRLS. Kaplan–Meier survival plot showed that patients in the high-risk groups exhibited shorter overall survival (OS) than those in low-risk groups ($P < 0.001$). Compared with clinical data, the area under curve (AUC) values of the risk factors, decision curve analysis (DCA), the AUC values of different years and multivariate Cox regression suggested that the signature had better predictive power. Gene set enrichment analysis (GSEA) revealed the potential pathways of 12 ferroptosis-related lncRNAs, including sphingolipid-metabolism, mTOR signaling pathway, notch signaling pathway, homologous recombination, endocytosis, cell cycle, etc. Immune microenvironment including tumor-infiltrating immune cells, immune-related functions, checkpoint-related genes and N6-methyladenosine (m6A)-related mRNA were also significantly different between the two risk groups.

Conclusions This study constructed 12 FRLS for HCC patients to predict survival, which may provide promising targets for the therapy of HCC.

Introduction

Hepatocellular carcinoma (HCC) ranks fifth in the incidence of malignancies and is the second leading cause of cancer-related deaths among men worldwide [1]. In China, due to factors such as hepatitis B and eating habits, there are 392,868 new HCC cases, resulting in 368,960 deaths during 2018, accounting for almost half of the global new cases and deaths of HCC [2]. HCC can be treated with surgical resection, liver transplantation, locoreginoal therapy and systemic therapy. Only few patients are diagnosed at early

stages when several treatment options such as surgical resection, transplantation, are effective. Most patients are diagnosed at middle-late stage due to the asymptomatic nature, outwith the criteria for surgical resection [3].For unresectable patients, tyrosine kinase inhibitors (TKIs), such as sorafenib and lenvatinib are applicable [4].However, the clinical researches showed that the median survival time for these two treatment is about one year [5], and both are associated with considerable side effects that impair quality of life. Immunotherapy, including anti-VEGF, anti-PD-1 strategies, may benefit HCC patients with sorafenib resistance or refractory [6, 7].A recent study showed that unresectable patients treated with PD-1 inhibitors combined with anti-VEGF therapies have a 1-year survival rate of only about 67%, better than patients treated with sorafenib [8]. The overall efficacy of HCC patients is unsatisfactory, and the 5-year overall survival (OS) rate is still below 20% [9]. Indeed, the high heterogeneity and the complexity of the tumor microenvironment (TME) lead to great differences in the sensitivity of individuals to the treatment [10], which requires more studies to understand its underlying mechanisms. At present, it has been found that treatments such as anti-PD-1 and sorafenib could induce ferroptosis [11, 12], a form of nonapoptotic regulated cell death (RCD) that differs from apoptosis, necroptosis and autophagy, caused by iron-dependent accumulation of lipid peroxide and reactive oxygen species (ROS) [13]. Researchers have found ferroptosis is involved in malignant tumors, such as HCC, renal cell carcinoma, non-small-cell lung carcinoma, ovarian cancer, et al [10, 14, 15]. Importantly,it is found that cancer cells are prone to ferroptosis when treated with some anti-tumor therapies [16], and there are numbers of pathways to regulate ferroptosis sensitivity, the functions of ferroptosis-inducing genes such as CISD1 [17] and ferroptosis-related genes such as Rb [18], NRF2 [19] and MT1G [20] are gradually known, which show new opportunities to treat therapy-insensitive tumors [21], studies on ferroptosis also dominate gradually.

Long non-coding RNAs (lncRNAs) refer to a type of non-coding RNAs with a length of more than 200 nucleotides, which are not translated into protein [22]. Studies indicated that lncRNAs participate in various physiological and pathological processes through interacting with DNA, mRNA, or proteins, thus associated with tumorigenesis and tumor development. For example, cytosolic lncRNA P53RRA induces ferroptosis and apoptosis by interacting with G3BP1(a modulator of Ras signaling pathway), resulting in greater retention of P53 in the nucleus [23].GABPB1-AS1 lncRNA aggravates oxidative stress by inhibiting cell antioxidant capacity in HepG2 cells [24]. However, there are still few studies that systematically illustrate the ferroptosis-related lncRNAs correlated with the prognosis of HCC. We constructed a prognostic ferroptosis-related lncRNAs signature (FRLS), which had a favorable predictive capability on the prognosis of HCC. In addition, we assessed the association between the prognostic FRLS and ferroptosis-related mRNA, immune microenvironment including the expression of tumor-infiltrating immune cells, immune-related functions, which might represent a new therapeutic frontier for cancer therapy.

Materials And Methods

Data collection

The RNA sequencing data and corresponding clinical data, including age, gender and survival information were acquired from The Cancer Genome Atlas (TCGA) database (https://portal.gdc.cancer.gov/), these data were updated to May 01, 2021.In addition, samples with survival time less than 30 days and incomplete clinical data were excluded. Since the data involved in this study all came from the TCGA database and strictly followed the TCGA publication guidelines (http://cancergenome.nih.gov/abouttcga/policies/publicationguidelines), no approval from the ethics committee is required.

Identification of ferroptosis-related lncRNAs

The RNA sequencing data was normalized and transformed using the formula $\log_2$. 245 ferroptosis-related genes were acquired from the Molecular Signature Database [25] (https://www.gsea-msigdb.org/gsea/msigdb/index.jsp). The ferroptosis-related differentially expressed genes (DEGs) between tumor tissues and adjacent nontumorous tissues were uncovered based on FDR < 0.05 and $|\log_2 FC|>1$, the Gene Ontology (GO) function analysis [26] including biological processes (BP), molecular functions (MF), and cellular components (CC) and the Kyoto Encyclopedia of genes and Genomes (KEGG) [27] analysis were performed to reveal the biological function of ferroptosis-related DEGs. Gene transfer format (GTF) files were obtained from Ensembl (http://asia.ensembl.org) to annotate and identify the lncRNAs. Pearson correlation analysis was carried out between the lncRNAs and ferroptosis-related genes with the |Correlation Coefficient| > 0.4 and P < 0.001.

Construction and validation of the prognostic FRLS

Firstly, ferroptosis-related lncRNAs involved in survival were selected by univariate Cox regression analysis (P < 0.0001). Lasso regression analysis were then performed to minimize the risk of overfitting. The results were integrated in the multivariate Cox regression analysis to determine whether the ferroptosis-related lncRNAs were independent prognosis predictors of HCC. Finally, we constructed a linear combination of risk scores based on ferroptosis-related lncRNAs expression profiles multiplied by regression coefficients: risk score = $\sum_{i=1}^{n}\beta_i * (\text{expression of lncRNA}_i)$.

Prediction accuracy of FRLS

According to the median risk score, patients were assigned into high- and low-risk groups. Kaplan-Meier survival analysis was conducted to assess the difference of OS between the two groups. The receiver operating characteristic curve (ROC), the area under the risk model curve (AUC), and decision curve analysis (DCA) [28] were utilized to assess the prediction accuracy of gene signature. What's more, univariate and multivariate Cox regression analyses were generated to evaluate the prognostic value of the risk score model and each clinicopathological features. The connection between ferroptosis-related lncRNAs and clinicopathological manifestations was exhibited by a heatmap.

Functional Enrichment Analysis

Principal component analysis (PCA) [29] and t-distributed stochastic neighbor embedding(t-SNE) [30] were performed to reduce dimension and determine the clustering ability of the FRLS. Besides, differences in potential biological course between the two groups were investigated by GSEA (http://www.broadinstitute.org/gsea/index.jsp), FDR < 0.25 and P < 0.05 were regarded as statistically significant.

Establishment of nomogram

Nomogram was established to predict the recurrence or death of HCC by using the rms R package. And calibration plots were drawn to estimate the predictive accuracy of the nomogram.

Evaluation of immune microenvironment

The TIMER [31],CIBERSORT [32], CIBERSORT-ABS, QUANTISEQ [33], MCP-counter [34], XCELL [35], EPIC [36] algorithms were used to assess the immune infiltration status between the two groups based on prognostic FRLS. The heatmap was utilized to visualize the differences in expression profiles of tumor-infiltrating immune cells under different algorithms. Single-sample gene set enrichment analysis (ssGSEA) algorithm was applied to analyze immune-related functions in the different groups.

Statistical analysis

Kaplan–Meier survival analysis and log-rank test were conducted to compare differences in OS between the different groups. Spearman correlation analyses were utilized to determine the correlation between two parameters. Benjamini-Hochberg method was performed to identify the differently expressed lncRNAs according to FDR. All statistical analyses were performed by R software 3.5.3. Statistical significance was set as the P < 0.05.

Results

The flow chart of this study was shown in Fig. 1. Finally, 424 HCC samples from the TCGA cohort were included, including 374 HCC tissues and 50 adjacent non-tumor tissues. Detailed clinical features are summarized in Table 1.

Table 1
The clinical features of HCC patients

Characteristics	Number
Age category < 65/≥65/NA	224/152/1
Sex Male/female	255/122
Follow-up state Alive/dead	128/249
Tumor stage I/II/III/IV/NA	175/87/86/5/24
Tumor grade G1/G2/G3/G4/NA	55/180/124/13/5
T stage T1/T2/T3/T4/NA	185/95/81/13/3
M stage M0/M1/NA	272/4/101
N stage N0/N1/NA	257/4/116

Enrichment Analysis of ferroptosis-related genes

84 ferroptosis-related DEGs, including 13 downregulated and 71 upregulated genes were uncovered(Fig S1A, S1B, Table S1).BP of target genes were enriched in response to oxidative stress, reactive oxygen species metabolic process, response to metal ion and metabolism of superoxides among others; CC were mainly enriched in the regulation of NADPH oxidase complex, oxidoreductase complex and melanosome among others; MF were mainly enriched in oxidoreductase activity acting on NAD(P)H, coenzyme binding, and ferric iron binding among others. KEGG analysis revealed the target genes participated in the regulation of the process of ferroptosis, synthesis of microRNAs in cancer cells, pathways of neurodegeneration-multiple diseases, central carbon metabolism in cancer cells, VEGF signaling pathway, HIF-1 signaling pathway, arachidonic acid metabolism, hepatocellular carcinoma, bladder cancer (Fig. 2A, 2B).

FigureS1 Expression profiles of ferroptosis-related DEGs with HCC. (A) Heatmap for ferroptosis-related DEGs with significant differences. (B) Volcano plot for ferroptosis-related DEGs, sky blue indicates

downregulated of genes, and light salmon indicates upregulated of genes

Construction of a prognostic model

After performing the lncRNA annotation file, we obtained 14142 lncRNAs in TCGA datasets (Table S2). Besides, 245 ferroptosis-related genes were retrieved from the Molecular Signature Database (Table S3). After performing the Pearson correlation analysis between the lncRNAs and ferroptosis-related genes. We obtained 1273 ferroptosis-related lncRNAs, and 784 of them (Table S4), including 17 downregulated and 767 upregulated ferroptosis-related lncRNAs were considered statistically significant (FDR < 0.05 and $|\log_2 FC|>1$, Fig. 3A, 3B). Univariate Cox regression analysis revealed 34 ferroptosis-related lncRNAs were significantly associated with prognosis (Fig. 4). These 34 ferroptosis-related lncRNAs were incorporated into the multivariate COX analysis. As shown in Table 2, 12 survival-related lncRNAs (LUCAT1, LINC01224, THUMPD3-AS1, AC116025.2, LINC00942, SNHG10, AC131009.1, POLH-AS1, MKLN1-AS, LINC01138, LNCSRLR, AL031985.3) were considered as independent prognosis predictors of HCC. Among them, AC116025.2 and THUMPD3-AS1 were favorable prognostic factors. To investigate the potential functions of the 12 ferroptosis-related lncRNAs, a visualization co-expression network of the 12 ferroptosis-related prognostic lncRNAs and ferroptosis-related genes was established (Fig. 5A-B). Finally, risk score based on the FRLS was generated.

Table 2
The risk model of 12 ferroptosis-related lncRNAs with prognostic value for HCC by multivariate Cox regression analysis

LncRNA _ symbol	HR	HR.95L	HR.95H	P-value	Coef
LUCAT1	1.150028974	1.029451792	1.284729068	0.013375922	0.139787137
LINC01224	1.482561097	1.045422785	2.102486609	0.027161969	0.393771063
THUMPD3-AS1	0.777056359	0.592693586	1.018766864	0.067938912	-0.252242397
AC116025.2	0.600897127	0.346926787	1.040788347	0.069168286	-0.509331528
LINC00942	1.03428835	1.013489738	1.055513787	0.001142753	0.033713606
SNHG10	1.207897103	1.020767523	1.429331731	0.027856511	0.188880916
AC131009.1	1.409501424	0.973537793	2.040695573	0.06907616	0.343236042
POLH-AS1	2.571170482	1.459614528	4.529221599	0.001078996	0.944361236
MKLN1-AS	2.00249721	1.109125488	3.615456607	0.021248057	0.694395007
LINC01138	1.238483258	0.975544653	1.572291721	0.078982627	0.213887452
LNCSRLR	2.299942704	1.456749121	3.631192472	0.000350805	0.832884211
AL031985.3	1.284205708	0.92833387	1.776499118	0.130835351	0.250140401

Survival results and multivariate examination

Based on the median risk score value, the patients were divided into high- and low-risk groups. As shown in Fig. 6A, Kaplan-Meier analyses showed the high-risk groups exhibited shorter OS than low-risk groups ($P < 0.001$). Based on the FRLS, the AUC of the signature was 0.817, showing superior performance to clinicopathological features in predicting the prognosis of HCC (Fig. 6B,6E). The survival status plot showed that the patients' risk score was inversely related to their survival rate (Fig. 6C). The AUC predictive value of the FRLS for 1, 3, 5-year survival rate was 0.817, 0.760 and 0.749, respectively (Fig. 6D). Besides, Fig. 6F indicated the expression profiles of the 12 lncRNAs were different between the high- and low-risk groups. Univariate and multivariate COX analysis revealed that the risk signature was an independent prognostic factor of HCC (Fig. 7A,7B). The heatmap for the association between FRLS and clinicopathological manifestations was also analyzed (Fig. 8). The nomogram indicated that the risk signature was the most important factor affecting the patients' survival, followed by tumor stage and T stage (Fig. 9A), the calibration plots of the nomogram revealed that the actual and predicted survival times of 1, 3, and 5 years were consistent (Fig. 9B-9D), which demonstrated that the nomogram using the prognostic FRLS was reliable.

Functional enrichment analysis

PCA and t-SNE revealed that the low- and high-risk groups exhibited distribution differences based on the risk signature and median risk score value, implying that the lncRNAs signature could divide HCC patients into two clusters and that the ferroptosis status of HCC patients was different between the low- and high-risk groups (Fig. 10). However, PCA showed that the groups did not exhibit a significant separation based on the whole genome and ferroptosis-related genes expression profile (Fig S2A, S2B). GSEA was further used to distinguish their potential functions in order to further determine the cause of the significant differences in survival rates between the two groups. Based on the criterion of a FDR P-value < 0.05, Fig. 11 indicated that ferroptosis and tumor-related pathways, including sphingolipid-metabolism, notch signaling pathway, mTOR signaling pathway, homologous recombination, endocytosis, cell cycle, non-small cell lung cancer, bladder cancer were enriched in the high-risk groups. Whereas, some metabolism-related signal pathways belonged to the low-risk groups, including degradation of valine, leucine and isoleucine, tryptophan metabolism, fatty acid metabolism, primary bile acid biosynthesis. By retrieving the PubMed database, we found that most of the prognostic ferroptosis-related lncRNAs were related to tumorigenesis and progression. The results also suggested the ferroptosis and carcinogenic statuses were different between the low- and high-risk groups.

FigureS2 PCA analysis. (A) PCA plot between high- and low-risk groups based on all genes. (B) PCA plot between high- and low-risk groups based on ferroptosis-related genes

Correlation of the risk signature and the immune microenvironment of HCC

We further explored the association between the risk signature and the immune microenvironment of HCC. The heatmap of immune infiltration based on multiple algorithms was shown in Fig. 12, which indicated that the risk signature was related to tumor-infiltrating immune cells. The ssGSEA algorithm was then used to compare the immune-related functions between high- and low-risk groups. Immune-

related functions including cytolytic activity, and type II IFN response were enriched in low-risk groups, but MHC class I response was enriched in high-risk groups ($P < 0.05$; Fig. 13A). Given the importance of checkpoint inhibitor-based immunotherapies, we further investigated the difference of immune checkpoints expression profile between different groups. We found that the expression of PDCD-1 (PD-1), NRP1, TNFSF4/9/15/18, CTLA4, TNFRST4/8/9/14/18/25 and ICOS et al were significantly different (Fig. 13B). The expression of m6A-related mRNA, including YTHDF1/2, YTHDC1/2, FTO, HNRNPC, RBM15, WTAP, METTL3/14 was also significantly different between high- and low- risk groups (Fig. 14). Altogether, the FRLS may be a candidate biomarker for HCC immunotherapy.

Discussion

HCC is characteristic of high malignancy and high mortality because of the heterogeneity of tumor microenvironment. Recently, although advances in treatment of HCC, the prognosis of patients with advanced HCC remains unsatisfactory. Indeed, the response of each HCC patients to drug treatments is quite different, due to molecular heterogeneity. Numerous studies have focused on ferroptosis, for it influences therapeutic vulnerabilities and may predict clinical outcomes [37]. In addition, it has been confirmed that ferroptosis plays a key role in HCC migration, invasion, proliferation, which provides a new angle for the therapy as well as prognosis for HCC [10]. Evidences have demonstrated that lncRNAs play a crucial regulatory role in cancer-associated ferroptosis process.

For instance, LncRNA MT1DP could aggravate oxidative stress in hepatocytes through interplay with miR-365, and as the intermediate to repress NRF2-mediated antioxidant signaling [38]. LINC01554 closely related to tumor invasion, tumor size, tumor staging and shorter survival of HCC, exerted its tumor-suppressive function

through regulating PKM2 and Akt/mTOR signaling pathway [39]. Although a few studies have indicated that ferroptosis-associated genes and lncRNAs might regulate drug-induced ferroptosis in HCC [22], their correlation with the prognosis of HCC patients remains undefined. In this study, we constructed 12 FRLS to predict OS of HCC patient. Meanwhile, we explored the relationship between the FRLS and immune microenvironment, for it can effectively predict the prognosis of patients. Therefore, this study proposes the potential biomarkers and therapeutic targets for HCC.

Firstly, 84 ferroptosis-related DEGs and 784 ferroptosis-related lncRNAs were obtained. KEGG analyses revealed the genes mainly participated in synthesis of microRNAs in cancer cells, central carbon metabolism in cancer cells, VEGF signaling pathway, HIF-1 signaling pathway. A recent study found that exosomal miR-522 derived from cancer-associated fibroblasts suppressed ferroptosis, and the knockdown of miR-522 could enhance sensitivity to drug [40]. iASPP (inhibitor of apoptosis-stimulating protein of p53) was found to inhibit ferroptosis through the Nrf2/HIF-1 signaling pathway, thus played protective roles in acute lung injury [41]. In this study, ferroptosis-related lncRNAs (LUCAT1, LINC01224, THUMPD3-AS1, AC116025.2, LINC00942, SNHG10, AC131009.1, POLH-AS1, MKLN1-AS, LINC01138, LNCSRLR, AL031985.3) were selected as independent prognostic factors for HCC. LUCAT1 over-

expressed in HCC and other malignant tumors, was found to associated with shorter OS [42] and as well regulate breast cancer stemness by activation of Wnt/β-catenin pathway [43]. LINC01224 enhanced the malignant phenotype of HCC cells by elevating expression of CHEK1 [44]. The high expression level of THUMPD3-AS1, significantly related to the progression and recurrence of NSCLC, regulated cancer cells self-renewal via miR-543 and ONECUT2 [45].LINC00942 (LNC942) elicited pro-tumorigenic roles

by promoting METTL14-mediated m6A methylation and subsequently enhancing the stability and expression of CXCR4 and CYP1B1 [46]. SNHG10, associated with poor OS of HCC, could facilitate the carcinogenesis and metastasis of HCC cells through modulating the expression of SCARNA13 [47]. MKLN1-AS highly expressed in HCC tissues, was reported to be associated with shorter OS, the knockdown of MKLN1-AS tremendously suppressed HCC cells proliferation, invasion, and migration [48].LINC01138 played a nonnegligible role in tumorigenicity and metastasis of HCC by activating PRMT5 [49]. LNCSRLR, involved in predicting the prognosis of patients of renal cell carcinoma, exerted its carcinogenic role by directly binding to NF-κB, thus leading to the development of intrinsic sorafenib tolerance [50]. However, to date, there is no study on the role of AC116025.2, AC131009.1, POLH-AS1, AL031985.3 in tumors, thus requires subsequent experiments.

The risk score of each HCC patient was calculated on the basis of the expression of the 12 prognostic ferroptosis-related lncRNAs and patients were grouped into low- or high-risk groups according to the median value of the risk score. The Kaplan-Meier curves showed that FRLS could distinguish the patients with good prognosis from those with poor prognosis ($P < 0.001$). The AUC predictive value of the FRLS corresponding to 1 year, 3 years, and 5 years of survival were 0.817, 0.760 and 0.749. Besides, the Cox regression analysis concluded that the signature is an independent factor of HCC. Combining the risk model and clinical value, such as age, gender, clinical stage, and TNM stage, we found that the FRLS was closely related to the malignant clinical-pathological characteristics of the samples. To further analyze these 12 lncRNAs of the signature, we established a nomogram and validated their predictive value. All above results indicated that this FRLS had superior prognostic value to clinicopathological factors. The results of PCA and t-SNE suggested that the significant difference in OS between the two groups might originate from different ferroptosis status induced by FRLS. GSEA analysis indicated that ferroptosis-related and tumor-related pathways, such as sphingolipid-metabolism, notch signaling pathway, mTOR signaling pathway, homologous recombination, endocytosis, cell cycle, non-small cell lung cancer, bladder cancer were enriched in the high-risk groups. Previous studies have shown that cell proliferation and cancer-related pathways have long been known to participate in ferroptosis regulation and progression of tumors [15, 51], thus affecting survival in patients with HCC. Furthermore, mTOR pathway has been confirmed to be involved in mediating ferroptosis in cancers cells, and inhibition of the PI3K-AKT-mTOR signaling pathway sensitizes cancer cells to ferroptosis induction [52]. On the other hand, the metabolism-related pathway belonged to the low-risk groups. Indole-3-pyruvate (I3P) was highly protective against ferroptosis by activation of anti-oxidative stress pathways, recently, interleukin-4-induced-1 (IL4i1) was reported to suppress ferroptosis by generating I3P from tryptophan [53].Besides, elongation of very long-chain fatty acid protein 5 (ELOVL5) and fatty acid desaturase 1 (FADS1) participated in regulating polyunsaturated fatty acid biosynthesis, lack of these enzymes rendered cells

resistant to ferroptosis [54].The results suggested that ferroptosis-associated lncRNAs strongly related to the biological characteristics of HCC progression, which may benefit future precision targeted therapy.

Recently, immunotherapy as a new paradigm of cancer treatment has attracted more attention. Considering immune microenvironment strongly associated with the process of hepatocarcinogenesis, proliferation, metastasis, and thus significantly influence cancer progression, immunotherapy response and patient prognosis. Researchers also have witnessed ferroptosis and lncRNAs play a crucial role in cancer progression and therapeutic effect via diverse biological ways. A few studies have evaluated the relation between immune checkpoint inhibitors and ferroptosis. Wang et al. [16] reported that CD8 + T cells activated by checkpoint inhibitors could regulate cancer cells ferroptosis through releasing IFN-γ and subsequently reducing the expression of SLC3A2 and SLC7A11. Lang et al. [55] also confirmed that immunotherapy based on immune checkpoint inhibitors can enhance antitumor activity by induction of ferroptosis. However, the potential molecular mechanisms linking the ferroptosis-related lncRNAs to cancer immunity remain to be further investigated. Herein, we utilized the lncRNAs-mRNA co-expression network to explore the function of related lncRNAs, which is of great significance to innovation of immunotherapy strategies. Besides, we further assessed the relative immune cell infiltration of each sample by using multiple algorithms. Results indicated that patients in the two risk groups exhibited different immune status, immune-related functions including cytolytic activity, type II IFN response and MHC class I responses were different significantly between the two groups ($P < 0.05$). Significant differences in the expression of immune checkpoints between high- and low-risk groups indicated the differences in the sensitivity to immunotherapies. which illustrated that targeting tumor-specific ferroptosis pathways in combination with immune checkpoint inhibitors is a promising regimen in the future, especially for the types with immune checkpoint inhibitors-resistant [56]. These results indicated that the prognostic signature was related to the immune microenvironment of HCC, should be taken into account in clinical treatment.

N6-methyladenosine (m6A), recognized as one of the most frequent chemical modifications that occurs in mRNAs and lncRNAs in many eukaryotic species, exerts important effects on RNA metabolism including translation, splicing, export, degradation and microRNA processing [57, 58]. It has been reported that m6A was closely associated with various biological pathways, including ferroptosis-related pathways and tumor-related pathways [59], thus played a nonnegligible role in the heterogeneity and complexity of the TME [60]. In the study, we found that the expression of m6A (YTHDF1/2, YTHDC1/2, FTO, HNRNPC, RBM15, WTAP, METTL3/14) was significantly different between the two risk groups, which may aid in development of personalized immunotherapy strategies.

Nowadays, limited issues have confirmed that some drugs and immunotherapies could induce ferroptosis, which serves as potential therapeutic strategy for tumor treatment. However, the interconnection between ferroptosis and the heterogeneity of TME and the prognosis of HCC remain unknown. In our study, we constructed prognostic FRLS, exhibiting robust ability in predicting survival outcomes of HCC patients. Nonetheless, several issues remained in this study. Firstly, the prognostic model needs to be verified in other studies to guarantee its robustness. Secondly, our results have not

been clinically verified, the reliability cannot be fully guaranteed. Finally, experimental studies including quantitative real-time PCR and flow cytometry are required to confirm our findings.

Conclusions

We established prognostic FRLS that could accurately predict the survival outcomes of HCC. Our study also suggested that these 12 ferroptosis-related lncRNAs are potential therapeutic target, and may present individualized predictions for prognosis of HCC.

Abbreviations

HCC Hepatocellular carcinoma

LncRNAs Long non-coding RNAs

FIRLs ferroptosis and iron-metabolism related LncRNAs

OS overall survival

AUC area under the curve

PCA principal component analysis

HR hazard ratios

CI confidence intervals

GO Gene ontology

KEGG Kyoto Encyclopedia of Genes and Genomes

TCGA The Cancer Genome Atlas

DCA decision curve analysis

GSEA Gene set enrichment analysis

m6A N6-methyladenosine

TME the tumor microenvironment

FDR false discovery rate

ssGSEA single-sample gene set enrichment analysis

Declarations

Ethics approval and consent to participate

Since all data was obtained from the database, no ethical consent was required.

Consent for publication

Not applicable.

Availability of data and materials

The datasets obtained during the current study are available in the TCGA.

Competing interests

The authors declare that they have no competing interests.

Funding

It was an unfunded study.

Authors' contributions

Xiangjin Hu designed, analyzed the study and wrote the manuscript; Sailun Wang, Jia Guo, and Fang Xiong collected the data; Jun Lv revised this manuscript. All authors read and approved the final manuscript.

Acknowledgements

We thank the researchers who developed the R package.

References

1. Bray F, Ferlay J, Soerjomataram I, et al. Global cancer statistics 2018: GLOBOCAN estimates of incidence and mortality worldwide for 36 cancers in 185 countries. CA Cancer J Clin. 2018;68(6):394–424.
2. Feng RM, Zong YN, Cao SM, et al. Current cancer situation in China: good or bad news from the 2018 Global Cancer Statistics? Cancer Commun (Lond). 2019;39(1):22.
3. Maluccio M, Covey A. Recent progress in understanding, diagnosing, and treating hepatocellular carcinoma. CA Cancer J Clin. 2012;62(6):394–9.
4. Llovet JMRS, Mazzaferro V, Hilgard P, Gane E, Blanc JF, de Oliveira AC, Santoro A, Raoul JL, Forner A, Schwartz M, Porta C, Zeuzem S, Bolondi L, Greten TF, Galle PR, Seitz JF, Borbath I, Häussinger D, Giannaris T, Shan M, Moscovici M, Voliotis D, Bruix J, SHARP Investigators Study Group. Sorafenib in Advanced Hepatocellular Carcinom. N Engl J Med. 2008;359(4):378–90.

5. Kudo M, Finn RS, Qin S, et al. Lenvatinib versus sorafenib in first-line treatment of patients with unresectable hepatocellular carcinoma: a randomised phase 3 non-inferiority trial. The Lancet. 2018;391(10126):1163–73.
6. Zhu H, Yang X, Zhao Y, et al. Efficacy of anti-PD-1 antibody SHR-1210 as second-line treatment in hepatocellular carcinoma patient with sorafenib resistance: A case report. Med (Baltim). 2019;98(20):e15755.
7. Zhang EL, Zhang ZY, Li J, et al. Complete Response to the Sequential Treatment with Regorafenib Followed by PD-1 Inhibitor in a Sorafenib-Refractory Hepatocellular Carcinoma Patient. Onco Targets Ther. 2020;13:12477–87.
8. Finn RS, Qin S, Ikeda M, et al. Atezolizumab plus Bevacizumab in Unresectable Hepatocellular Carcinoma. N Engl J Med. 2020;382(20):1894–905.
9. Lu LC, Cheng AL, Poon RT. Recent advances in the prevention of hepatocellular carcinoma recurrence. Semin Liver Dis. 2014;34(4):427–34.
10. Nie J, Lin B, Zhou M, et al. Role of ferroptosis in hepatocellular carcinoma. J Cancer Res Clin Oncol. 2018;144(12):2329–37.
11. Li ZJ, Dai HQ, Huang XW, et al. Artesunate synergizes with sorafenib to induce ferroptosis in hepatocellular carcinoma. Acta Pharmacol Sin. 2021;42(2):301–10.
12. Jiang Z, Lim SO, Yan M, et al. (2021) TYRO3 induces anti-PD-1/PD-L1 therapy resistance by limiting innate immunity and tumoral ferroptosis. *J Clin Invest* 131(8).
13. Capelletti MM, Manceau H, Puy H, et al. (2020) Ferroptosis in Liver Diseases: An Overview. *Int J Mol Sci* 21(14).
14. Mou Y, Wang J, Wu J, et al. Ferroptosis, a new form of cell death: opportunities and challenges in cancer. J Hematol Oncol. 2019;12(1):34.
15. Yu H, Guo P, Xie X, et al. Ferroptosis, a new form of cell death, and its relationships with tumourous diseases. J Cell Mol Med. 2017;21(4):648–57.
16. Wang W, Green M, Choi JE, et al. CD8(+) T cells regulate tumour ferroptosis during cancer immunotherapy. Nature. 2019;569(7755):270–4.
17. Yuan H, Li X, Zhang X, et al. CISD1 inhibits ferroptosis by protection against mitochondrial lipid peroxidation. Biochem Biophys Res Commun. 2016;478(2):838–44.
18. Louandre C, Marcq I, Bouhlal H, et al. The retinoblastoma (Rb) protein regulates ferroptosis induced by sorafenib in human hepatocellular carcinoma cells. Cancer Lett. 2015;356(2 Pt B):971–7.
19. Sun X, Ou Z, Chen R, et al. Activation of the p62-Keap1-NRF2 pathway protects against ferroptosis in hepatocellular carcinoma cells. Hepatology. 2016;63(1):173–84.
20. Sun X, Niu X, Chen R, et al. Metallothionein-1G facilitates sorafenib resistance through inhibition of ferroptosis. Hepatology. 2016;64(2):488–500.
21. Friedmann Angeli JP, Krysko DV, Conrad M. Ferroptosis at the crossroads of cancer-acquired drug resistance and immune evasion. Nat Rev Cancer. 2019;19(7):405–14.

22. Jiang N, Zhang X, Gu X, et al. Progress in understanding the role of lncRNA in programmed cell death. Cell Death Discov. 2021;7(1):30.
23. Mao C, Wang X, Liu Y, et al. A G3BP1-Interacting lncRNA Promotes Ferroptosis and Apoptosis in Cancer via Nuclear Sequestration of p53. Cancer Res. 2018;78(13):3484–96.
24. Qi W, Li Z, Xia L, et al. LncRNA GABPB1-AS1 and GABPB1 regulate oxidative stress during erastin-induced ferroptosis in HepG2 hepatocellular carcinoma cells. Sci Rep. 2019;9(1):16185.
25. Subramanian A, Tamayo P, Mootha VK, et al. Gene set enrichment analysis: a knowledge-based approach for interpreting genome-wide expression profiles. Proc Natl Acad Sci U S A. 2005;102(43):15545–50.
26. Pomaznoy M, Ha B, Peters B. GOnet: a tool for interactive Gene Ontology analysis. BMC Bioinformatics. 2018;19(1):470.
27. Kanehisa M, Furumichi M, Tanabe M, et al. KEGG: new perspectives on genomes, pathways, diseases and drugs. Nucleic Acids Res. 2017;45(D1):D353-d61.
28. Simonsohn U, Simmons JP, Nelson LD. Specification curve analysis. Nat Hum Behav. 2020;4(11):1208–14.
29. Konishi T, Matsukuma S, Fuji H, et al. Principal Component Analysis applied directly to Sequence Matrix. Sci Rep. 2019;9(1):19297.
30. Kobak D, Berens P. The art of using t-SNE for single-cell transcriptomics. Nat Commun. 2019;10(1):5416.
31. Li T, Fan J, Wang B, et al. TIMER: A Web Server for Comprehensive Analysis of Tumor-Infiltrating Immune Cells. Cancer Res. 2017;77(21):e108-e10.
32. Newman AM, Liu CL, Green MR, et al. Robust enumeration of cell subsets from tissue expression profiles. Nat Methods. 2015;12(5):453–7.
33. Finotello F, Mayer C, Plattner C, et al. Molecular and pharmacological modulators of the tumor immune contexture revealed by deconvolution of RNA-seq data. Genome Med. 2019;11(1):34.
34. Becht E, Giraldo NA, Lacroix L, et al. Estimating the population abundance of tissue-infiltrating immune and stromal cell populations using gene expression. Genome Biol. 2016;17(1):218.
35. Aran D, Hu Z, Butte AJ. xCell: digitally portraying the tissue cellular heterogeneity landscape. Genome Biol. 2017;18(1):220.
36. Racle J, de Jonge K, Baumgaertner P, et al. (2017) Simultaneous enumeration of cancer and immune cell types from bulk tumor gene expression data. *Elife* 6(.
37. Kim J, DeBerardinis RJ. Mechanisms and Implications of Metabolic Heterogeneity in Cancer. Cell Metab. 2019;30(3):434–46.
38. Gao M, Li C, Xu M, et al. LncRNA MT1DP Aggravates Cadmium-Induced Oxidative Stress by Repressing the Function of Nrf2 and is Dependent on Interaction with miR-365. Adv Sci (Weinh). 2018;5(7):1800087.

39. Zheng YL, Li L, Jia YX, et al. LINC01554-Mediated Glucose Metabolism Reprogramming Suppresses Tumorigenicity in Hepatocellular Carcinoma via Downregulating PKM2 Expression and Inhibiting Akt/mTOR Signaling Pathway. Theranostics. 2019;9(3):796–810.
40. Zhang H, Deng T, Liu R, et al. CAF secreted miR-522 suppresses ferroptosis and promotes acquired chemo-resistance in gastric cancer. Mol Cancer. 2020;19(1):43.
41. Li Y, Cao Y, Xiao J, et al. Inhibitor of apoptosis-stimulating protein of p53 inhibits ferroptosis and alleviates intestinal ischemia/reperfusion-induced acute lung injury. Cell Death Differ. 2020;27(9):2635–50.
42. Xing C, Sun SG, Yue ZQ, et al. Role of lncRNA LUCAT1 in cancer. Biomed Pharmacother. 2021;134:111158.
43. Zheng A, Song X, Zhang L, et al. Long non-coding RNA LUCAT1/miR-5582-3p/TCF7L2 axis regulates breast cancer stemness via Wnt/β-catenin pathway. J Exp Clin Cancer Res. 2019;38(1):305.
44. Gong D, Feng PC, Ke XF, et al. (2020) Silencing Long Non-coding RNA LINC01224 Inhibits Hepatocellular Carcinoma Progression via MicroRNA-330-5p-Induced Inhibition of CHEK1. *Mol Ther Nucleic Acids* 19(482 – 97.
45. Hu J, Chen Y, Li X, et al. THUMPD3-AS1 Is Correlated With Non-Small Cell Lung Cancer And Regulates Self-Renewal Through miR-543 And ONECUT2. Onco Targets Ther. 2019;12:9849–60.
46. Sun T, Wu Z, Wang X, et al. LNC942 promoting METTL14-mediated m(6)A methylation in breast cancer cell proliferation and progression. Oncogene. 2020;39(31):5358–72.
47. Lan T, Yuan K, Yan X, et al. LncRNA SNHG10 Facilitates Hepatocarcinogenesis and Metastasis by Modulating Its Homolog SCARNA13 via a Positive Feedback Loop. Cancer Res. 2019;79(13):3220–34.
48. Gao W, Chen X, Chi W, et al. Long non–coding RNA MKLN1–AS aggravates hepatocellular carcinoma progression by functioning as a molecular sponge for miR–654–3p, thereby promoting hepatoma–derived growth factor expression. Int J Mol Med. 2020;46(5):1743–54.
49. Li Z, Zhang J, Liu X, et al. The LINC01138 drives malignancies via activating arginine methyltransferase 5 in hepatocellular carcinoma. Nat Commun. 2018;9(1):1572.
50. Xu Z, Yang F, Wei D, et al. Long noncoding RNA-SRLR elicits intrinsic sorafenib resistance via evoking IL-6/STAT3 axis in renal cell carcinoma. Oncogene. 2017;36(14):1965–77.
51. Fan Z, Wirth AK, Chen D, et al. Nrf2-Keap1 pathway promotes cell proliferation and diminishes ferroptosis. Oncogenesis. 2017;6(8):e371.
52. Yi J, Zhu J, Wu J, et al. Oncogenic activation of PI3K-AKT-mTOR signaling suppresses ferroptosis via SREBP-mediated lipogenesis. Proc Natl Acad Sci U S A. 2020;117(49):31189–97.
53. Zeitler L, Fiore A, Meyer C, et al. (2021) Anti-ferroptotic mechanism of IL4i1-mediated amino acid metabolism. *Elife* 10(.
54. Lee JY, Nam M, Son HY, et al. Polyunsaturated fatty acid biosynthesis pathway determines ferroptosis sensitivity in gastric cancer. Proc Natl Acad Sci U S A. 2020;117(51):32433–42.

55. Lang X, Green MD, Wang W, et al. Radiotherapy and Immunotherapy Promote Tumoral Lipid Oxidation and Ferroptosis via Synergistic Repression of SLC7A11. Cancer Discov. 2019;9(12):1673–85.
56. Tang R, Xu J, Zhang B, et al. Ferroptosis, necroptosis, and pyroptosis in anticancer immunity. J Hematol Oncol. 2020;13(1):110.
57. Liu N, Pan T. N6-methyladenosine–encoded epitranscriptomics. Nat Struct Mol Biol. 2016;23(2):98–102.
58. Huang H, Weng H, Chen J. m(6)A Modification in Coding and Non-coding RNAs: Roles and Therapeutic Implications in Cancer. Cancer Cell. 2020;37(3):270–88.
59. He L, Li H, Wu A, et al. Functions of N6-methyladenosine and its role in cancer. Mol Cancer. 2019;18(1):176.
60. Yu ZL, Zhu ZM. Comprehensive analysis of N6-methyladenosine -related long non-coding RNAs and immune cell infiltration in hepatocellular carcinoma. Bioengineered. 2021;12(1):1708–24.

Figures

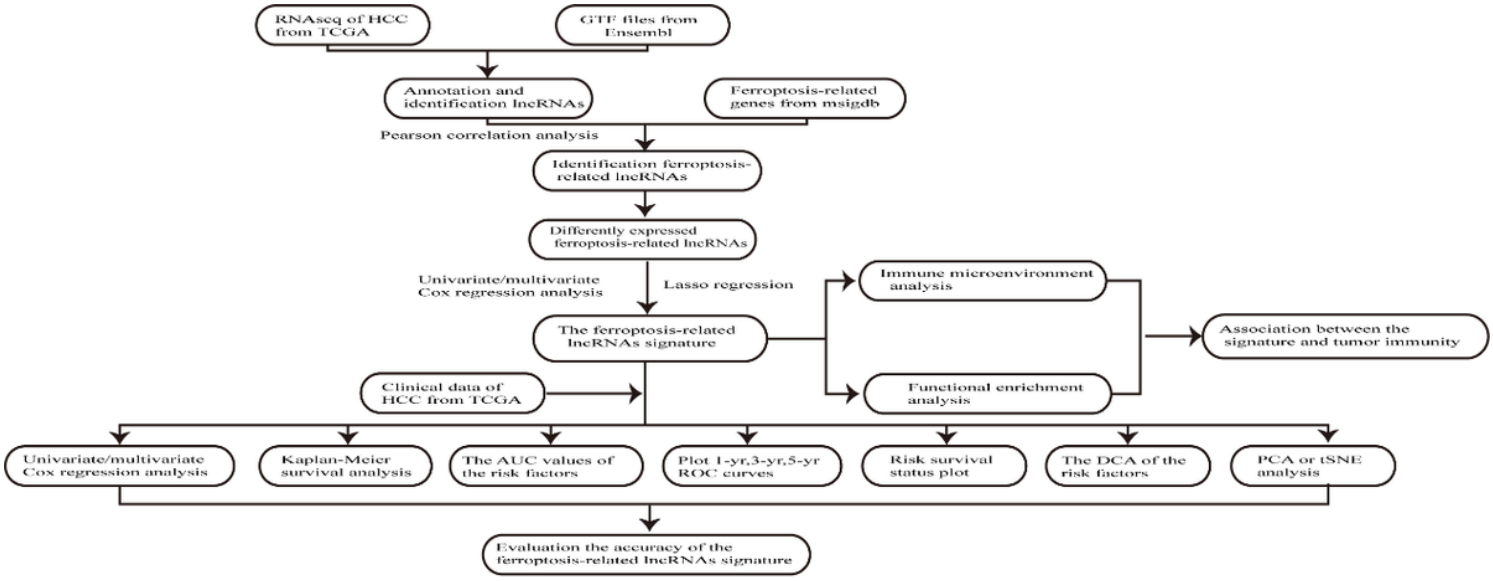

Figure 1

Flowchart of study design

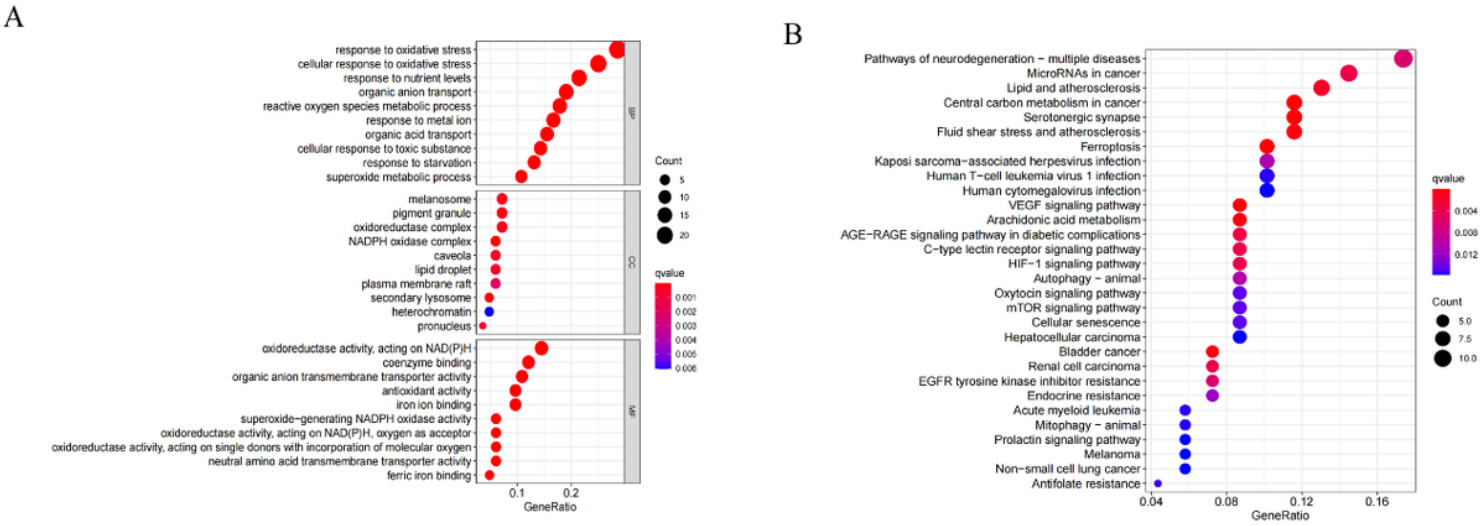

Figure 2

GO and KEGG analyses for ferroptosis-related DEGs. (A) GO and (B) KEGG

Figure 3

Expression profiles of ferroptosis-related lncRNAs with statistical significance of HCC. (A) Heatmap for ferroptosis-related lncRNAs with significant differences. (B)Volcano plot for ferroptosis-related differently expressed lncRNAs. Sky blue indicates downregulated of lncRNAs, and light salmon indicates upregulated of lncRNAs

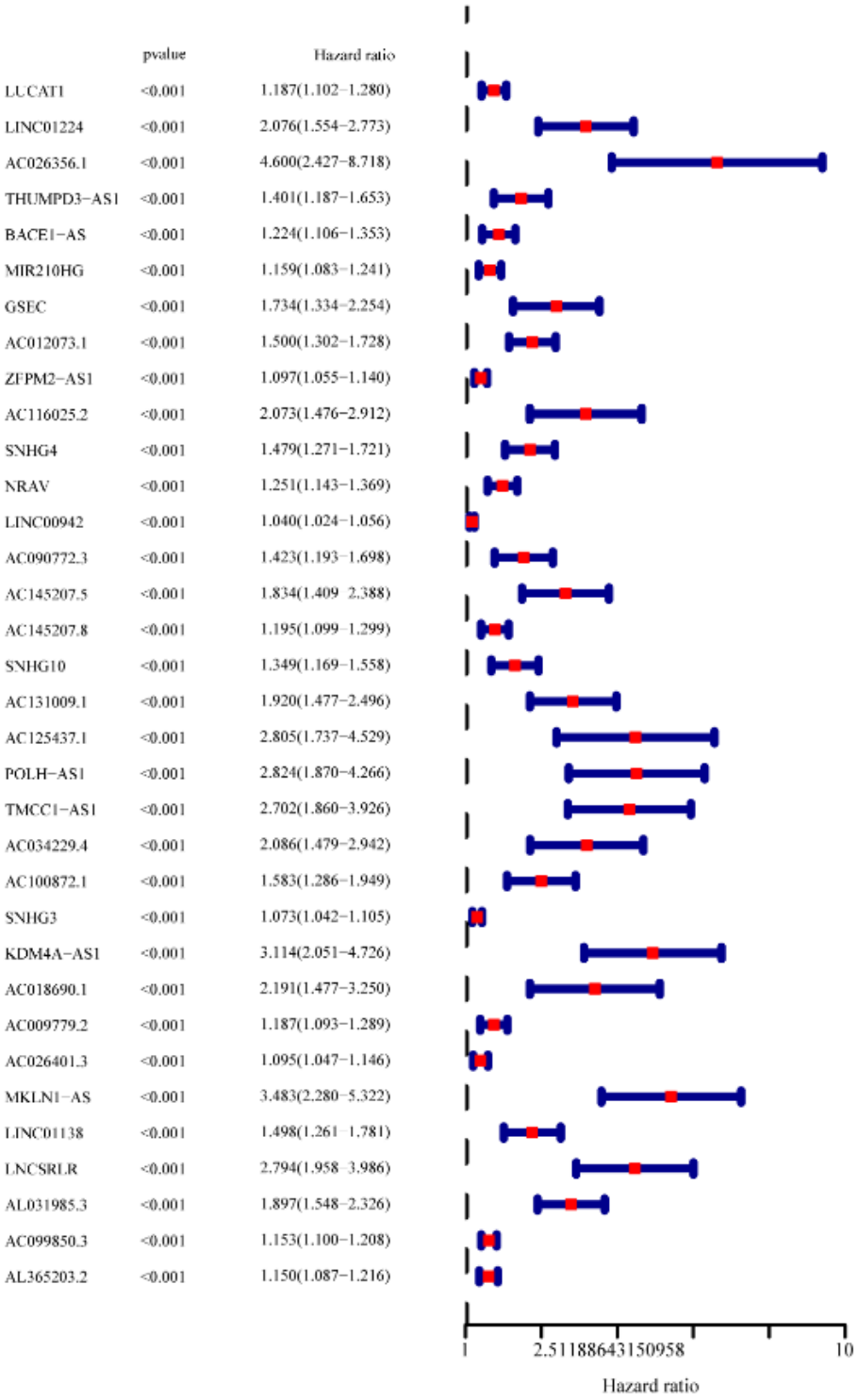

Figure 4

Univariate Cox regression analysis for the expression of 34 ferroptosis-related lncRNAs with the prognostic value

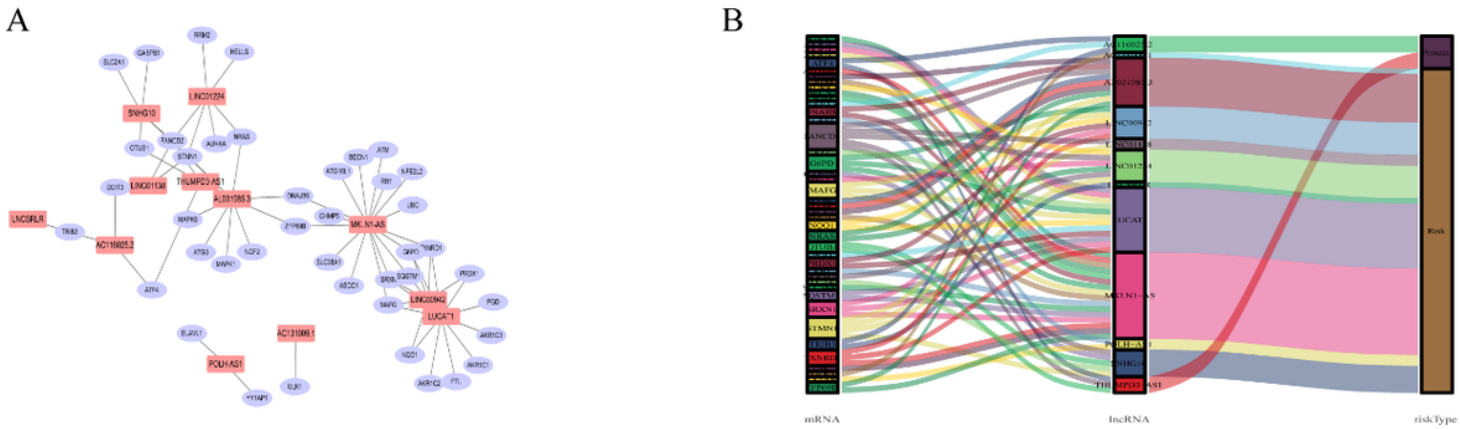

Figure 5

A co-expression network of the 12 ferroptosis-related lncRNAs-mRNA with prognostic value was visualized by Cytoscape and Sankey diagram. (A) Cytoscape. (B)Sankey diagram

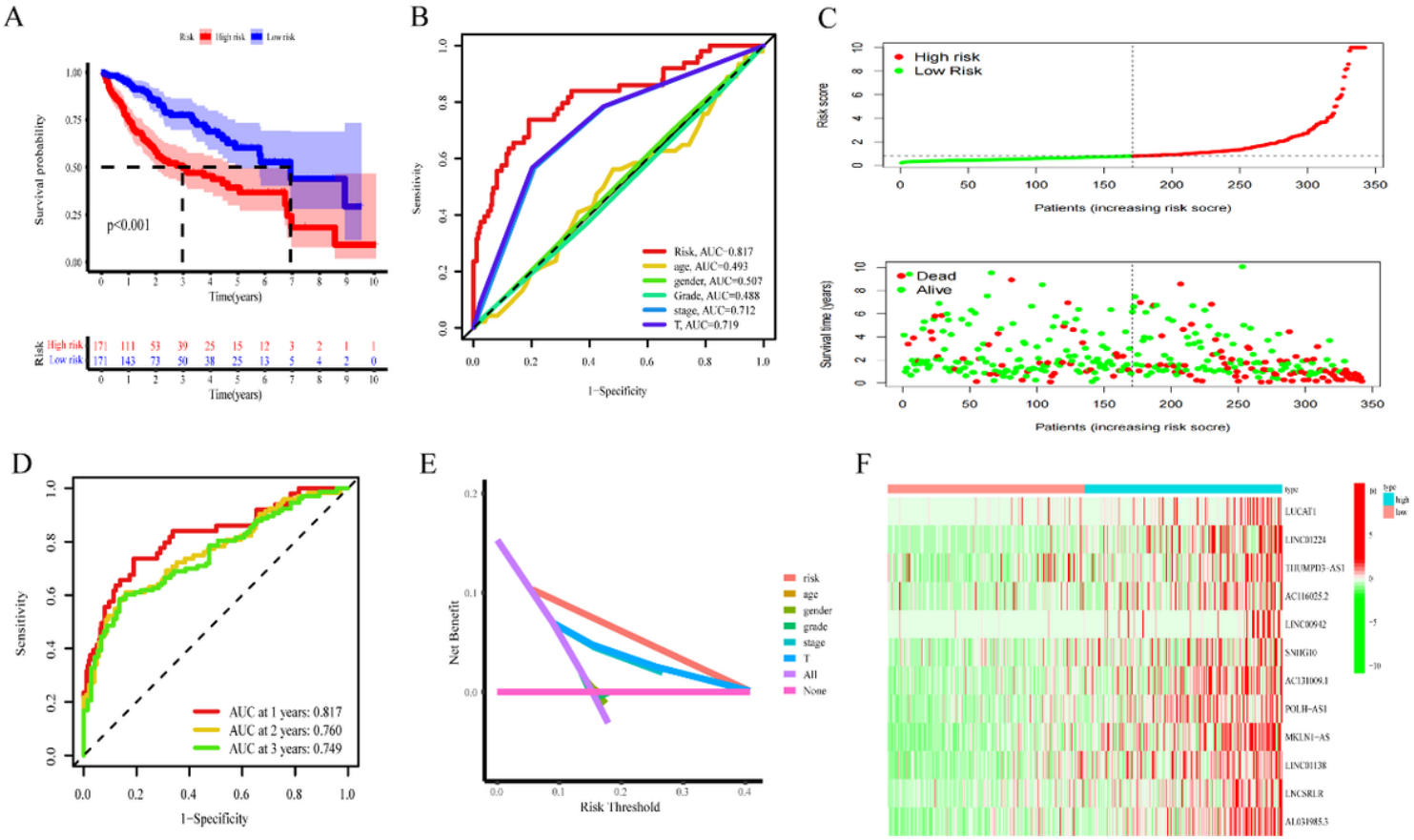

Figure 6

Evaluate the accuracy of the FRLS based on TCGA. (A) Kaplan-Meier survival analysis of the high- and low-risk groups on the basis of risk model and median risk score. (B) The AUC values for risk signature and clinical characteristics based on the ROC curves. (C) The distribution plots of the risk score and survival status. (D) The AUC of ROC analysis to predict the 1, 3, 5-year OS of HCC. (E)The DCA of the risk

model score and clinical characteristics. (F)The heatmap for the expression profiles of ferroptosis-related lncRNAs between the high- and low-risk groups

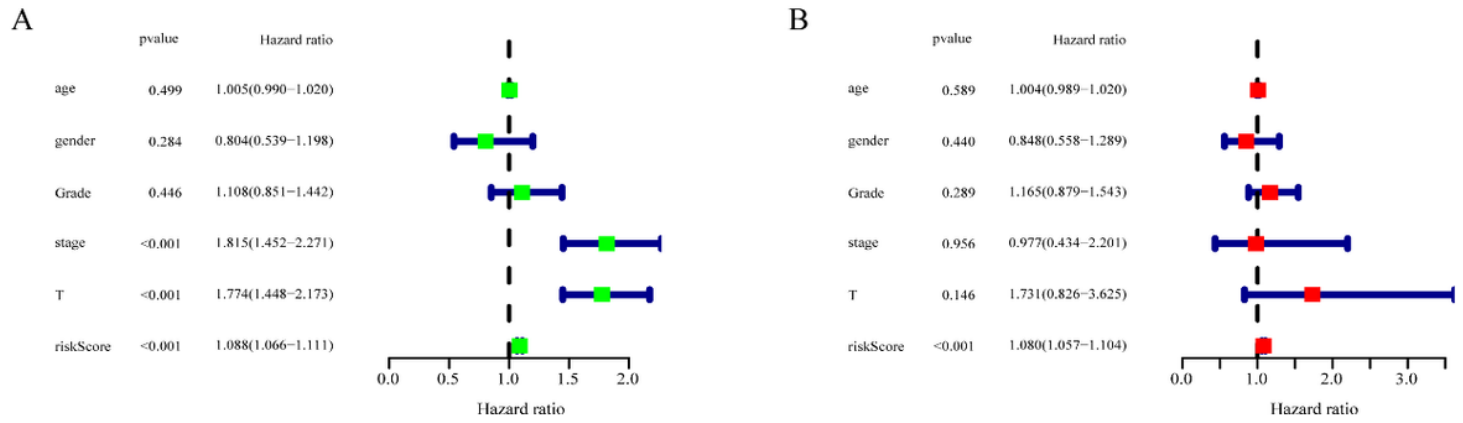

Figure 7

Assessment of prognostic value of the risk model in HCC. (A) The univariate Cox regression analysis for risk signature and clinical features. (B)The multivariate Cox regression analysis for risk signature and clinical features

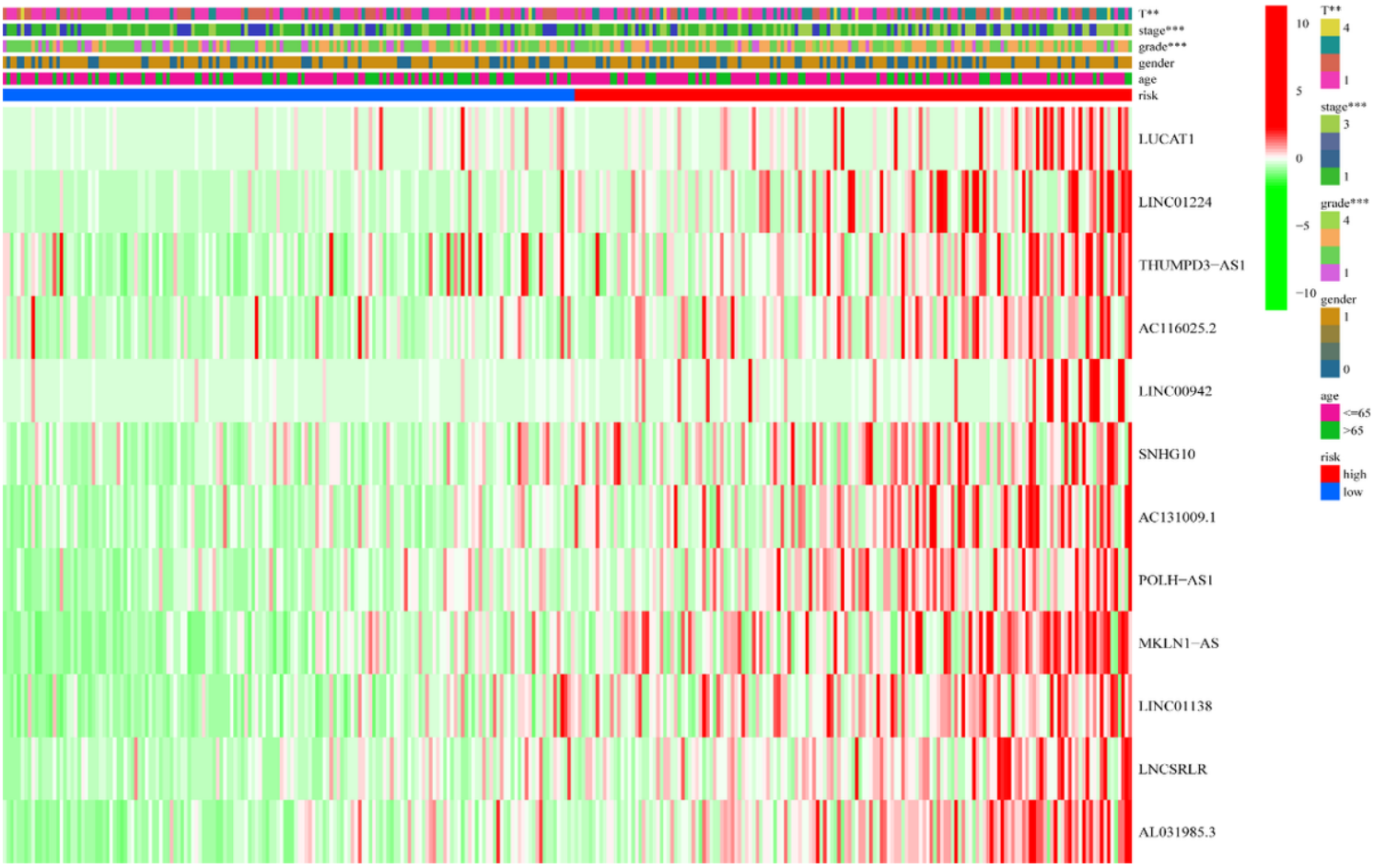

Figure 8

Heatmap of the clinicopathological characteristics and lncRNAs expression based on the risk score

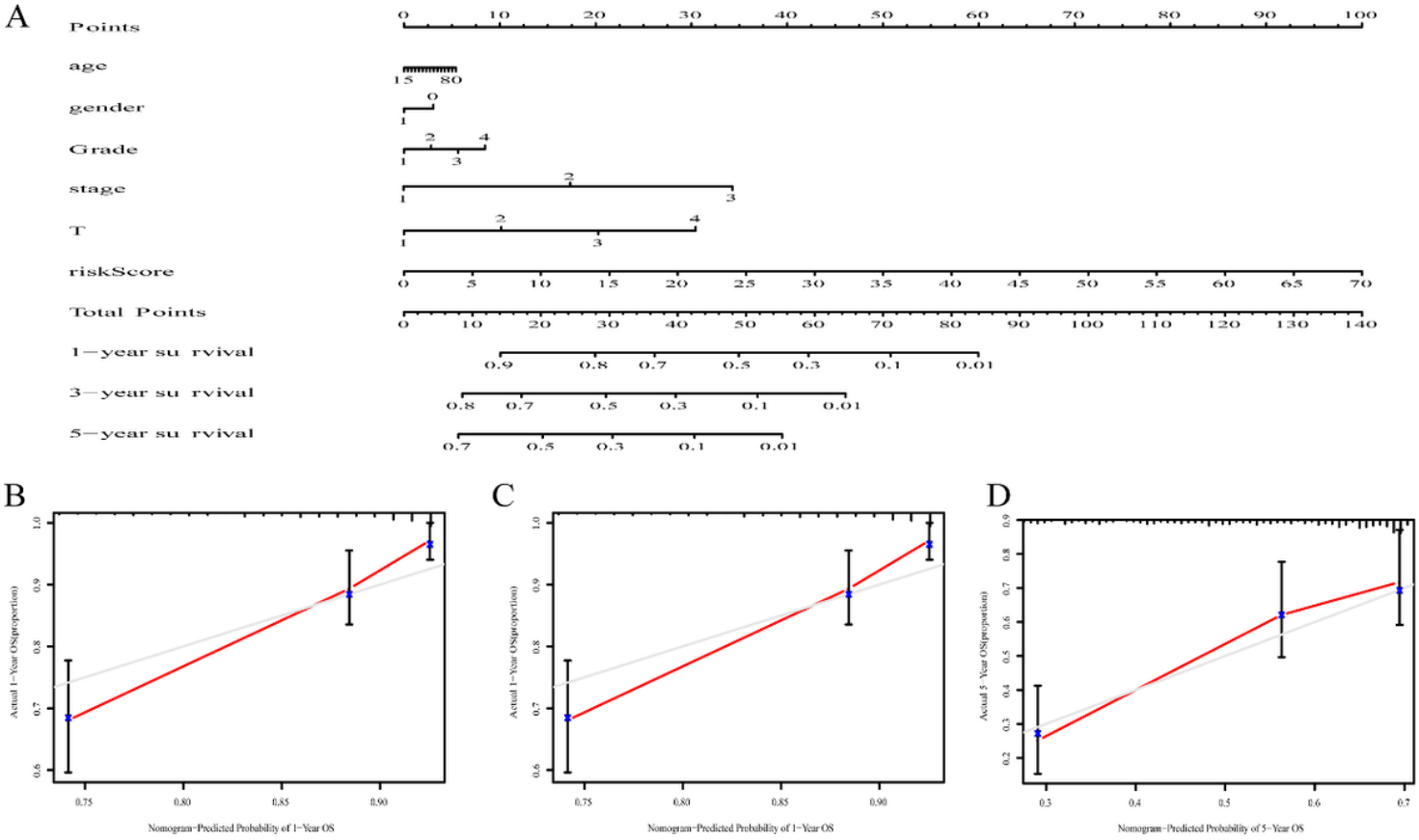

Figure 9

Establishment and assessment of a nomogram. (A) Nomogram based on risk signature, age and WHO grade. (B–D) Calibration curves for predicting 1-, 3-, and 5-year OS

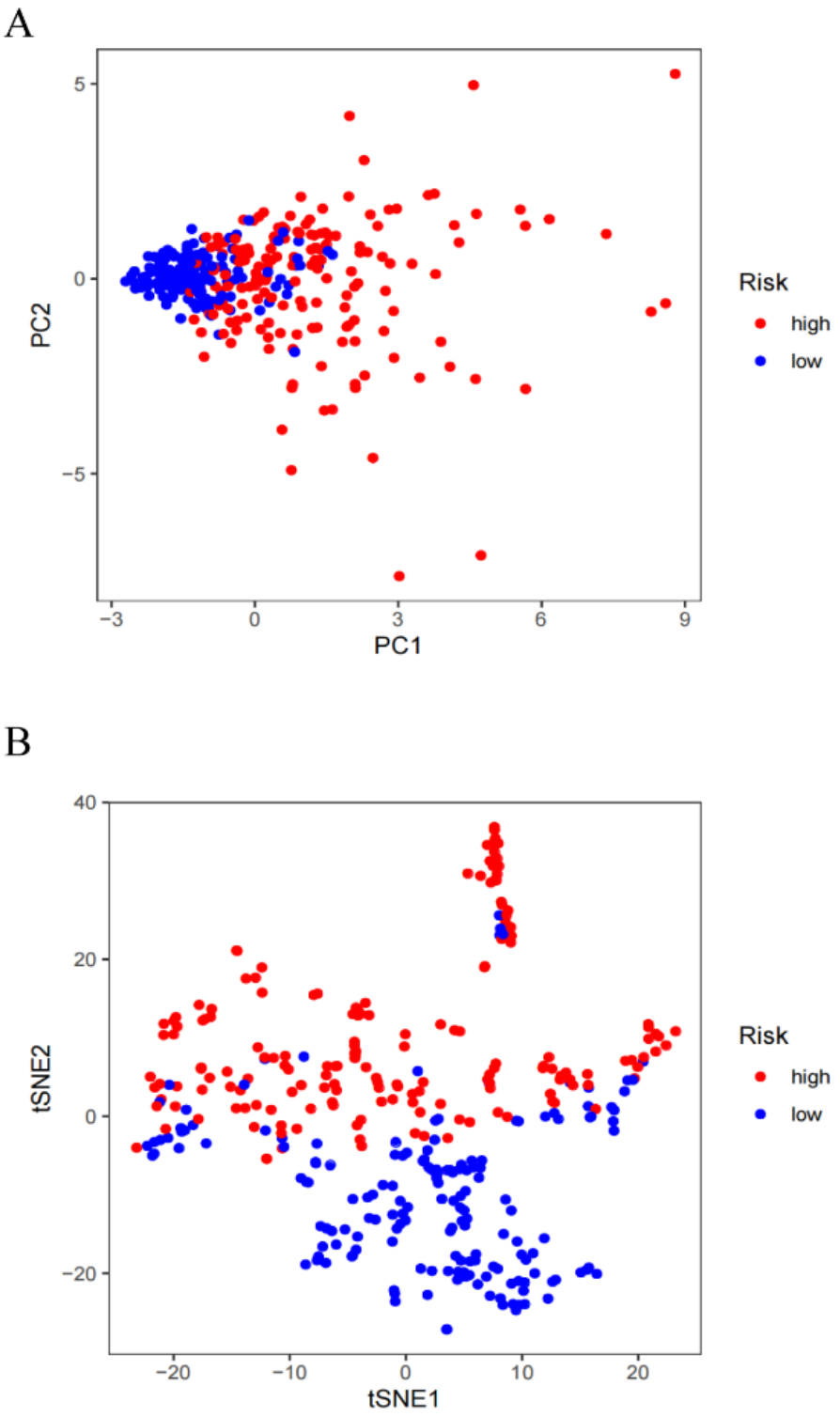

Figure 10

PCA and t-SNE between high- and low-risk groups based on the FRLS

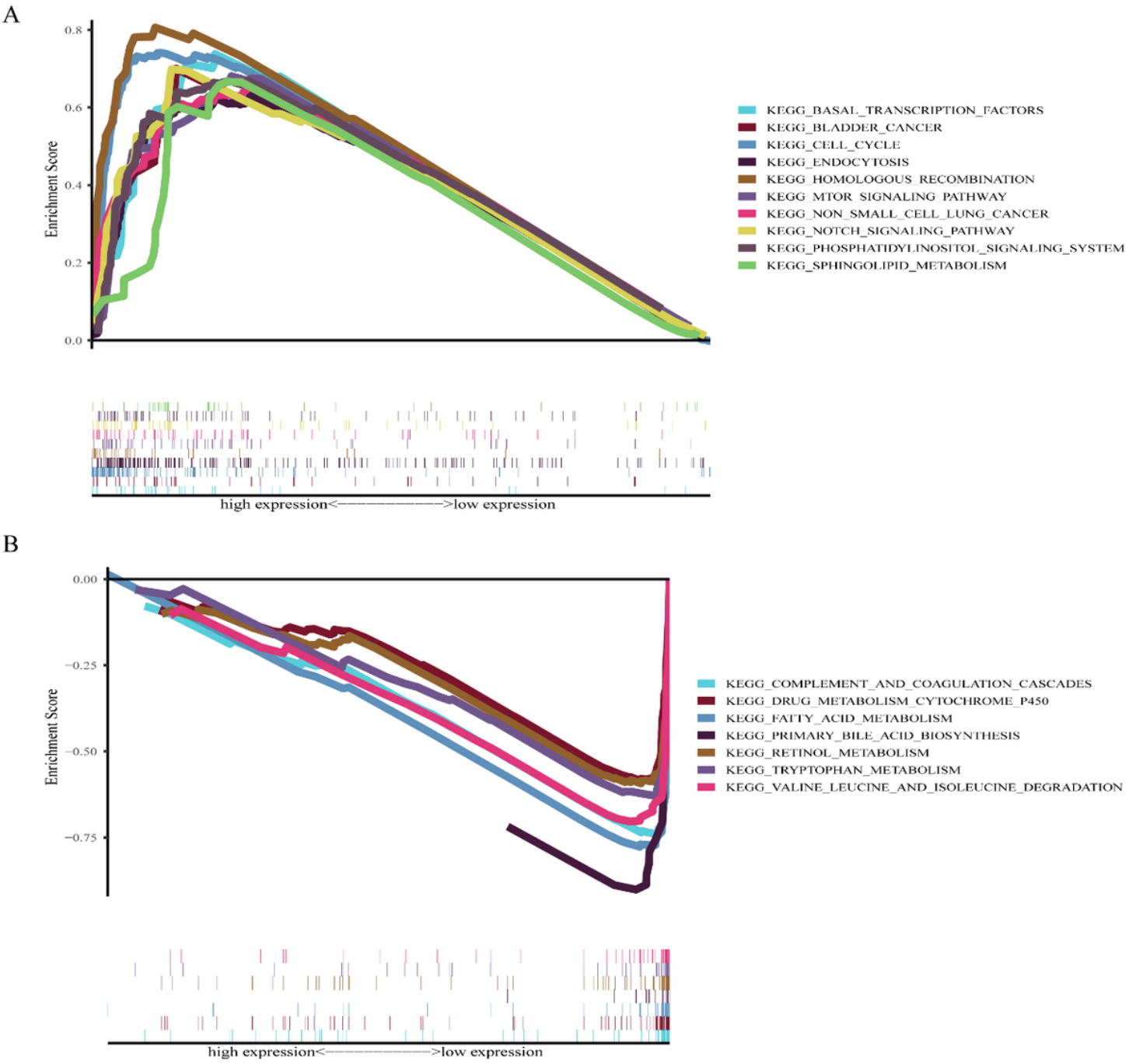

Figure 11

Gene set enrichment analysis. (A) Differentially regulated pathways in the high-risk groups. (B) Differentially regulated pathways in the low-risk groups

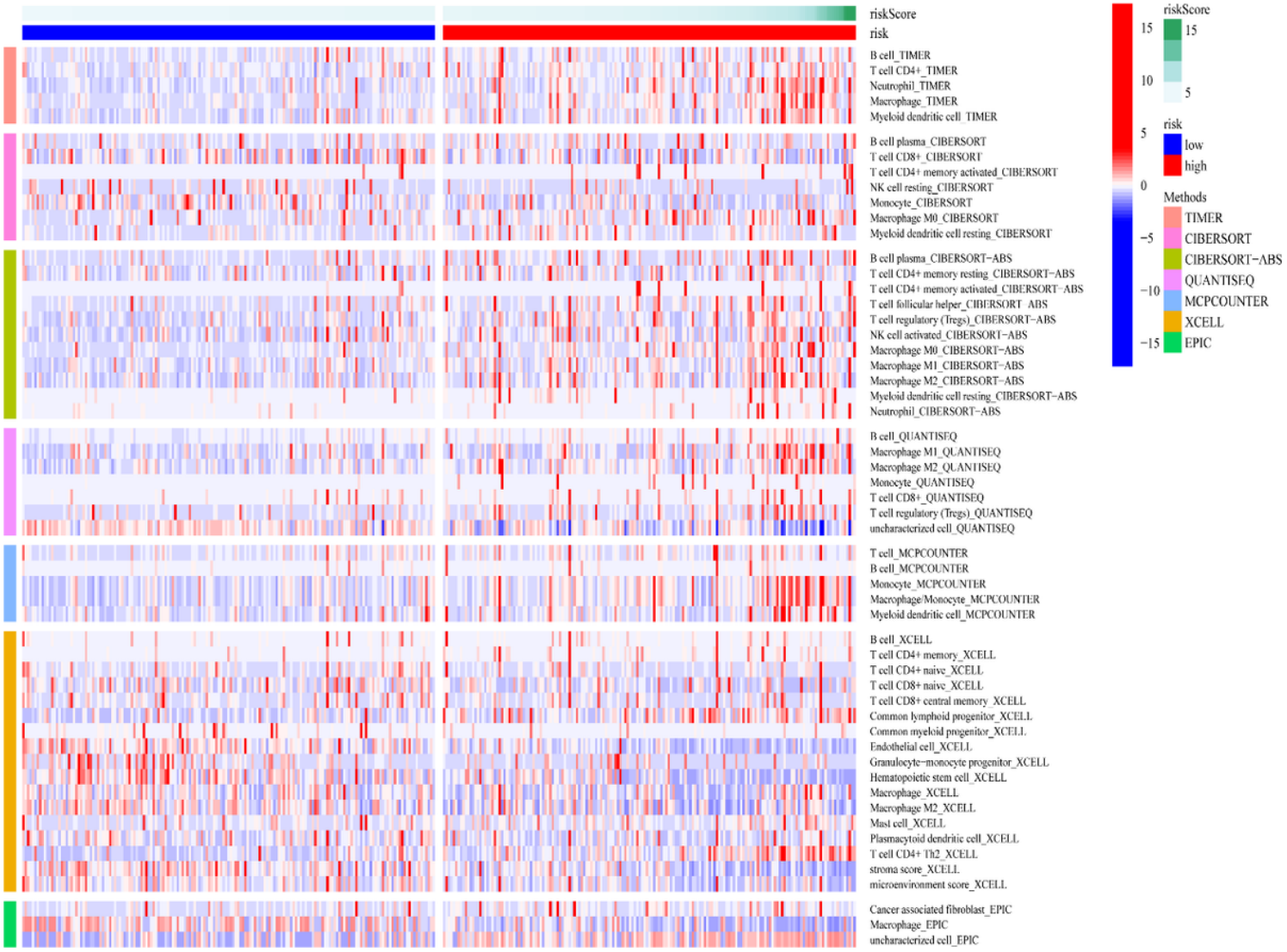

Figure 12

The heatmap of tumor-infiltrating immune cells between low- and high-risk groups on the basis of FRLS

A

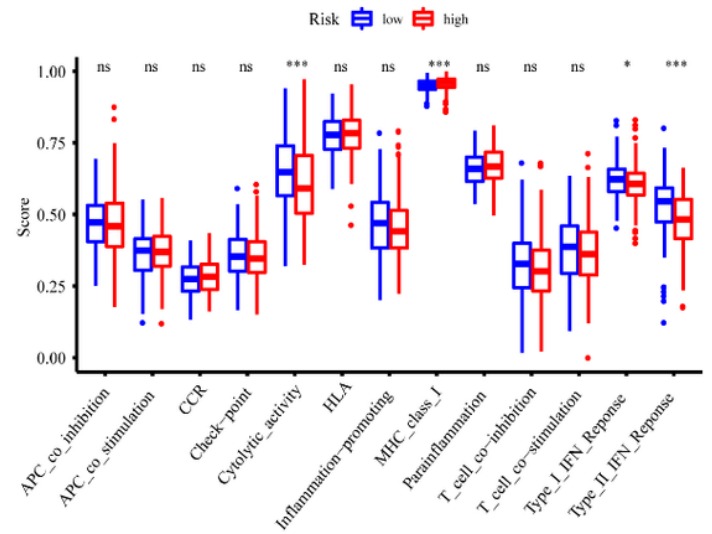

B

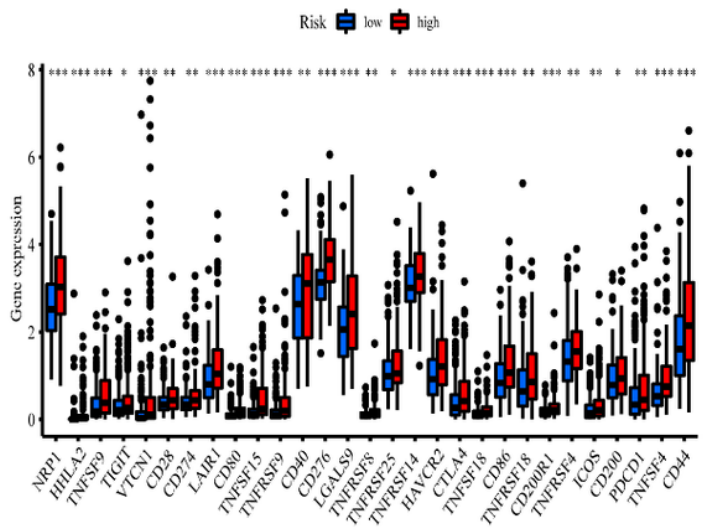

Figure 13

Immune infiltration analysis. (A)The expression profiles of immune-related functions based on ssGSEA between low- and high-risk groups. (B) The expression profiles of immune checkpoints between the low- and high-risk groups

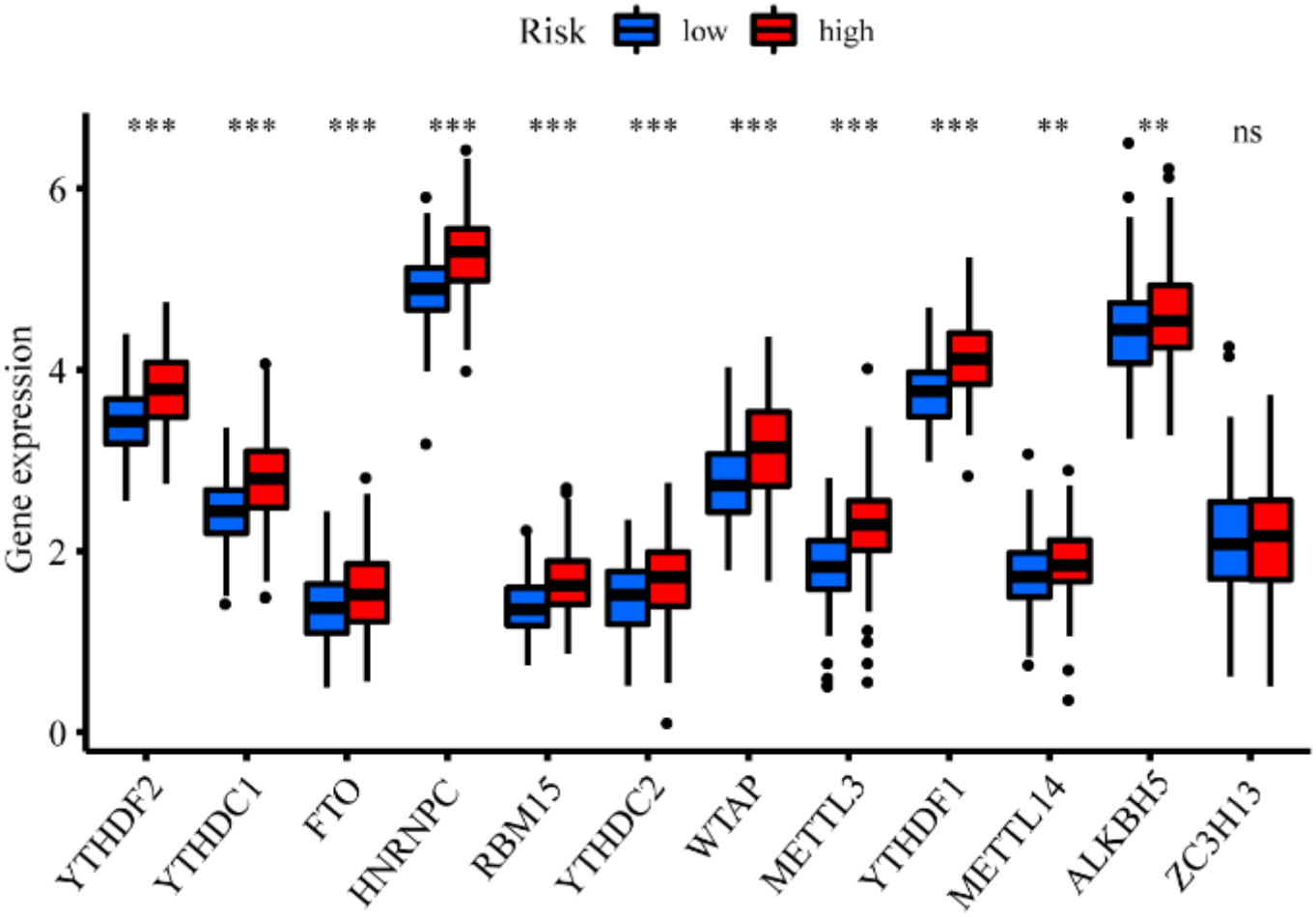

Figure 14

The expression of m6A-related genes between the two groups

Supplementary Files

This is a list of supplementary files associated with this preprint. Click to download.

- TABLES1.xls
- TABLES2.xls
- TABLES3.xls
- TABLES4.xls

- S1.png
- S2.png